

3-(diethylamino)-1-phenylpropan-1-one as a Corrosion Inhibitor for N80 Steel in Acidization of Petroleum Exploitation

Hu Wang^{1,2}, Yushuang Liu, Juan Xie¹, Junlei Tang^{2,3,*}, Ming Duan^{2,3,*}, Yingying Wang³,
Mohamad Chamas³

¹ School of Materials Science and Engineering, Southwest Petroleum University, Chengdu 610500, P.R.China

² State key Laboratory of Oil and Gas Reservoir Geology and Exploitation, Southwest Petroleum University, Chengdu 610500, P.R.China

³ School of Chemistry and Chemical Engineering, Southwest Petroleum University, Chengdu 610500, P.R.China

*E-mail: junleitang@126.com

Received: 22 March 2016 / Accepted: 15 April 2016 / Published: 4 May 2016

In this paper, the inhibiting performances of an acidizing corrosion inhibitor of 3-(diethylamino)-1-phenylpropan-1-one (Mannich base, MB) for N80 steel in 15% HCl solution was investigated using electrochemical and weight loss measurements. Polarization curves showed that MB inhibitor is a mixed-type corrosion inhibitor, which inhibits both the anodic and cathodic process of corrosion reaction. In addition, an apparent passivation region can be observed at anodic curves in the presence of high concentrations of MB, indicating a stronger barrier film at the interface. EIS also showed different pattern in different concentrations. Two capacitive impedance loop and two time constants, occurred at high MB concentrations, indicates two electrochemical kinetic processes at the interface, corrosion electrochemical process and the inhibitor film. Weight loss results showed that the MB inhibitor is highly efficient at all test temperatures. Activation energy and free energy obtained by fitting of the weight loss data proved that the adsorption of MB inhibitor is a complex mixed type, both physisorption and chemisorptions. SEM further proved MB inhibitor is highly efficient in inhibiting corrosion of N80 in HCl solution.

Keywords: Corrosion inhibitor; Hydrochloride acid; N80 steel; Polarization; EIS

1. INTRODUCTION

Corrosion extensively exists in many industrial applications. In most circumstances, corrosion is detrimental. Corrosion brings about direct or indirect economic loss, endangers the safety, wastes the

resources, pollutes the environment, and so on. However, there still exists some beneficiary that corrosion brings about. Printed circuit technique has been widely used electronic industry. That is the most commonly reminded example for the beneficiary of corrosion to a corrosion worker. Other examples are very rare and hard to be thought of by us. While in petroleum exploitation, a very specialized technique has been commonly applied for decades of years. It is called acidization, which is the example of both detrimental and beneficial of corrosion [1- 4].

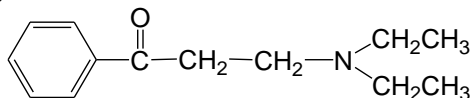
As an effective process for enhancing oil recovery, acidification is widely used in oil exploitation. In application, high concentration of acid solution is pumped into the stratum to corrode the rock. Hence due to the corrosion reaction between acid and rock, the pathway of oil is enlarged. As a consequence, the oil productivity is promoted. High concentration of hydrochloride acid (HCl), hydrofluoric acid (HF) or the mixture of the both acids is commonly used as acidification acid. HCl is commonly used for carbonatite and HF is usually used for silicate rocks. Mild steels, like N80, and some stainless steels are usually used as oil production tube. The inner wall of tubing steel tends to suffer from severe corrosion for high temperature, high pressure and strong acid in acidization process. In some extreme circumstances, the temperature in the bottom of the oil well can be more than 200°C and the pressure mounts to 100MPa. The use of excellent corrosion inhibitor is inevitable in preventing the tubing steel in acidization process [5-7].

Corrosion inhibitors for acid environment have been extensively studied. Many chemicals have been utilized as acidizing corrosion inhibitors [8-10]. In the early years, inorganic corrosion inhibitors were used as acidizing corrosion inhibitors, like chromate, nitrite and arsenide. While, these inhibitors are not in use anymore for the insufficiency in corrosion inhibition or high toxicity. Organic corrosion inhibitors containing groups of nitrogen, oxygen, sulfur and phosphorus are commonly used as practical acidizing corrosion inhibitors. The inhibition mechanism of the organic compounds can be expressed as the interactions between organic molecules and the metal surface via an adsorption process. Adsorption process of organic inhibitors on the metal surface is considered to happen according to physical adsorption or chemisorptions. The adsorption type can be determined by thermodynamic and kinetic parameters obtained from experimental data. Experimental data from electrochemical measurements and weight loss measurements have been extensively used to obtain the adsorption thermodynamic and kinetic parameters and to elucidate the inhibition mechanism [11-14].

Mannich base, based on Mannich reaction for synthesis, have been widely used as acidizing corrosion inhibitor both in laboratory and industrial application[15]. Aldehyde, alkynol and nitrogen containing compounds are usually used as high efficient corrosion inhibitors in acidification. Besides, the compound of ketone, aldehyde and amine condensation, one kind of Mannich base, is a good corrosion inhibitor with excellent performance and with very wide application. The application of ketone, aldehyde and amine condensation compound in acidization is very wide but the research on it is relatively few. In this paper, a typical mannich base (MB), 3-(diethylamino)-1-phenylpropan-1-one, was synthesized and its corrosion inhibition efficiency was also studied by weight loss, electrochemical measurements and SEM. The inhibition mechanism of the corrosion inhibitor in HCl solution was also discussed.

2. EXPERIMENTAL

A mixture of paraformaldehyde, diethylamine and acetophenone were refluxed in 130°C for 4h. The product, 3-(diethylamino)-1-phenylpropan-1-one (Mannich base, MB), was purified and characterized by FT-IR spectroscopy. The chemical structure of the inhibitor is shown as follows.



The aggressive solution (15% HCl) was prepared by dilution of analytical grade 38% HCl with double distilled water.

N80 specimen containing C=0.028%, Mn=1.48%, Si=0.17%, S=0.026%, P=0.015, Mo=0.1%, Cr=0.2% and Al=0.007% was used for the experiments. Rectangular specimens with the size of 40 mm × 10 mm × 2 mm were used in weight-loss measurements. The specimens were polished with emery paper up to 1000 grade, rinsed with acetone and double distilled water. In weight loss measurement, the specimens were immersed into the acidic solution for 4 hours without stirring. After the experiment, the corrosion products were removed by chemical method and the weight loss was calculated. The corrosion inhibition of inhibitor was defined by the following expression:

$$\eta = \frac{CR_0 - CR}{CR_0} \times 100\% \quad (1)$$

where η is the corrosion inhibition efficiency. CR_0 and CR are the corrosion rate in the absence and presence of the corrosion inhibitor, respectively.

All the reagents used in the measurements are analytical grade and prepared by deionized water. The weight loss experiments were carried out at temperatures of 303K, 323K, 343K and 363K, respectively.

The electrochemical measurements were carried out by IVIUMSTAT ELECTROCHEMICAL INTERFACE (IVIUM TECHNOLOGIES, Netherlands). The work electrode of N80 was coated with epoxy resin and with only 1cm² of the surface area exposed to solution. The reference electrode was saturated calomel electrode (SCE) and platinum bar was used as counter electrode. In polarization curve measurement, the scanning started from -0.250V (vs. open circuit potential, OCP) and ended at +0.250V (vs. OCP) with a scanning rate of 0.3 mV/s. The corrosion inhibition efficiency was calculated by the equation:

$$\eta = \frac{I_{\text{corr}(0)} - I_{\text{corr}(1)}}{I_{\text{corr}(0)}} \times 100\% \quad (2)$$

where η is the corrosion inhibition efficiency. $I_{\text{corr}(0)}$ and $I_{\text{corr}(1)}$ are corrosion current densities in the absence and presence of MB inhibitor.

In electrochemical impedance spectroscopy measurement, the amplitude of the alternative current was ±10mV and the measurement conducted at the open circuit potential. The frequency ranged from 10⁵ Hz to 10⁻¹ Hz. All the electrochemical measurements were carried out at 363K.

The surface morphologies without and with corrosion inhibitor were compared by scanning electronic microscopy (SEM, Cambridge s250 MK). The samples for SEM were from the weight loss experiments.

3. RESULTS AND DISCUSSION

3.1 Potentiodynamic polarization studies

The potentiodynamic polarization curves of N80 in the absence and presence of different concentrations of MB inhibitor are shown in Fig. 1 and the corresponding electrochemical parameters, including corrosion potential (E_{corr}), Tafel constants (b_a and b_c), corrosion current density (I_{corr}) and inhibition efficiency (η), are also shown in Table 1.

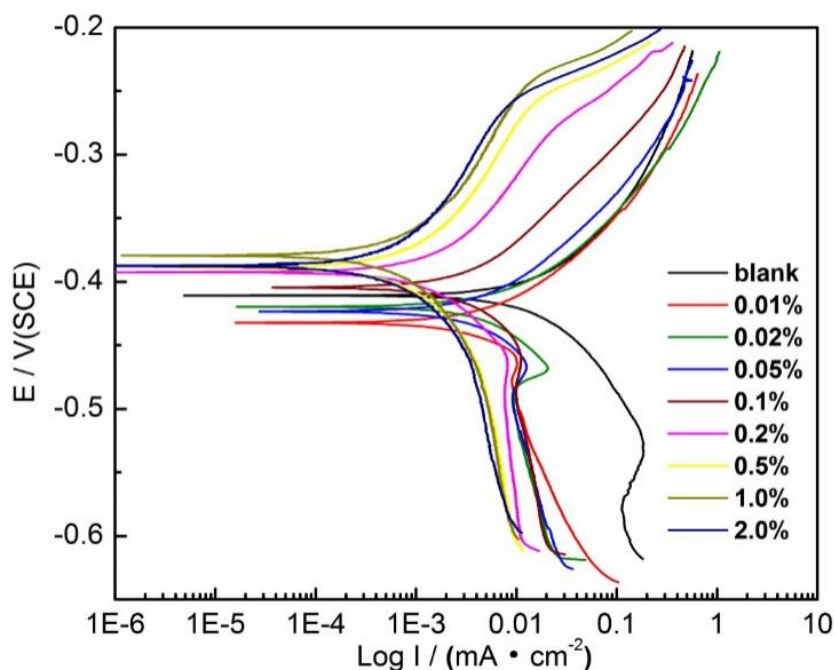


Figure 1. Polarization curves of N80 in 15% HCl at 363K in the absence and presence of different concentrations of MB

Table 1. Electrochemical parameters from polarization curves of N80 steel in 15% HCl in the absence and presence of MB inhibitor

C (w.t %)	E_{corr} (mV)	I_{corr} (mA cm ⁻²)	b_a (mV dec ⁻¹)	b_c (mV dec ⁻¹)	η (%)
0	-411	13.07	23	56	-
0.01	-432	3.59	28	60	72.57
0.02	-420	3.52	44	43	73.11
0.05	-423	2.74	52	44	79.03
0.1	-405	2.73	75	62	79.14
0.2	-393	1.22	73	75	90.67
0.5	-388	0.94	78	113	92.84
1	-378	0.52	81	98	95.98
2	-387	0.65	88	114	95.02

It is shown in Fig. 1 that the presence of MB inhibitor remarkably influences the polarization curves. In cathodic polarization curves, current peak in the middle of the cathodic region occurs in low

concentration, while such peak does not appear at higher concentration. It indicates the competitive adsorption process, possibly between Cl⁻ and MB molecules, occurs at this region. While in higher concentrations, such peaks disappear, indicating such competitive adsorption is no more existed. Anodic polarization curves also exhibit differently with the concentration of MB inhibitor. In the absence and low concentrations of MB, the anodic polarization curves behave as active dissolution. However, in higher concentration (above 0.2%), the passivation can be spotted, and the higher of the concentration, more apparent of the passive region. It reveals that, in low concentration of MB, hydrogen depolarization dominates without much inhibition. While in high concentration, MB film forms on the interface as a barrier to separate corrosive media from metal. Hence, the anodic dissolution has been reduced and hydrogen evolution reaction retarded.

Electrochemical parameters obtained from fitting also prove the inhibition behavior of MB inhibitor, shown in Table 1. It is generally assumed that the shifting direction of corrosion potential represents the electrochemical types of corrosion inhibitor when adding corrosion inhibitor. Positive shifting often stands for anodic corrosion inhibitor, in which the anodic process of corrosion has been inhibited in this circumstance. While negative shifting always means cathodic inhibitor, in which cathodic reaction of corrosion has been inhibited. Mixed type of corrosion inhibitor, both the anodic and cathodic process of corrosion has been inhibited, generally exists in many organic corrosion inhibitors. It can be seen from Table 2 that with the increase of the concentration of MB inhibitor, the E_{corr} is randomly changed. Moreover, the Tafel constants (b_a and b_c) increase with the concentration. It is generally believed that the inhibitor can be regarded as cathodic or anodic type when the shifting of corrosion potential is more than 85mV [16]. In our study, the maximum shifting of E_{corr} is 34mV towards anodic region. It indicates that MB is a mixed type inhibitor. Corrosion current density (I_{corr}) demonstrates that MB is highly efficient in inhibiting corrosion of N80 steel.

Table 2. Electrochemical parameters of EIS fitted by experimental data according to equivalent circuits of Fig.4.

MB conc. (%)	$R_s(\Omega \text{ cm}^2)$	$R_t(\Omega \text{ cm}^2)$	n	CPE($\mu\text{F cm}^{-2}$)	R_t'	CPE' ($\mu\text{F cm}^{-2}$)
blank	0.43	36.80	0.84	299	-	-
0.01	0.28	37.91	0.73	712	-	-
0.02	0.31	50.91	0.70	931	-	-
0.05	0.30	91.50	0.68	931	-	-
0.1	0.51	177.40	0.57	1632	-	-
0.2	0.11	54.65	0.60	1160	152.7	260
0.5	0.13	68.01	0.57	1025	290.5	257
1	0.10	86.51	0.57	1036	312.1	173
2	0.12	61.23	0.56	986	414.1	299

Remarkable alleviation of corrosion can be achieved even adding low concentration of MB inhibitor. The corrosion inhibition efficiency of MB inhibitor amounts to more than 90% when the concentration is higher than 0.2%.

3.2 Electrochemical impedance measurements

The inhibition performance of inhibitor at various concentrations of MB on N80 steel was studied by EIS measurements at 363K after 0.5h immersion time. Typical Nyquist plots are presented in Fig. 2.

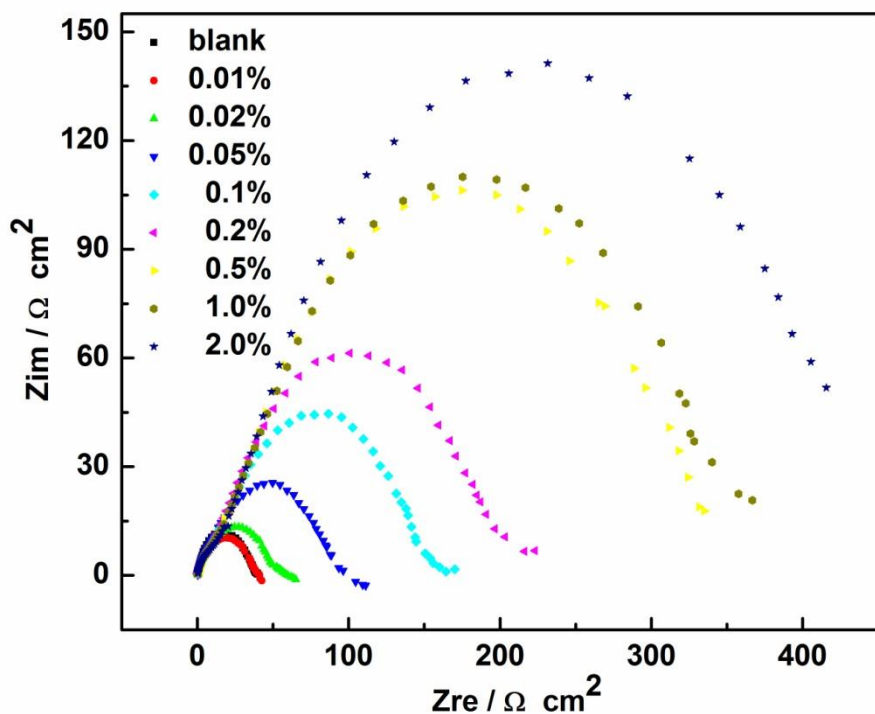


Figure 2. EIS Nyquist plots of N80 steel in 15% HCl solution at 363K in the absence and presence of different concentrations of MB

The magnitude of the impedance increases continuously with concentrations of MB inhibitor. All experimental plots have depressed capacitive semicircular over the studied frequency range, which is commonly attributed to the charge transfer reaction and the influence of roughness and other inhomogeneities of the surface [19-23]. The impedance spectra contain one or two capacitive loop, depending on the concentration of MB. Fig. 3 presents the impedance diagrams in the Bode formats of $|z|$ vs. frequency and phase angle vs. frequency. It can be observed from the phase angle changes that there exists one time constant only in the absence and presence of low concentrations of MB (below 0.1%). While in higher concentration (above 0.1%), two capacitive loop and two time constants can be seen from Fig. 2 and Fig. 3b, which indicates a more complex adsorption film comes into being in high concentration of MB.

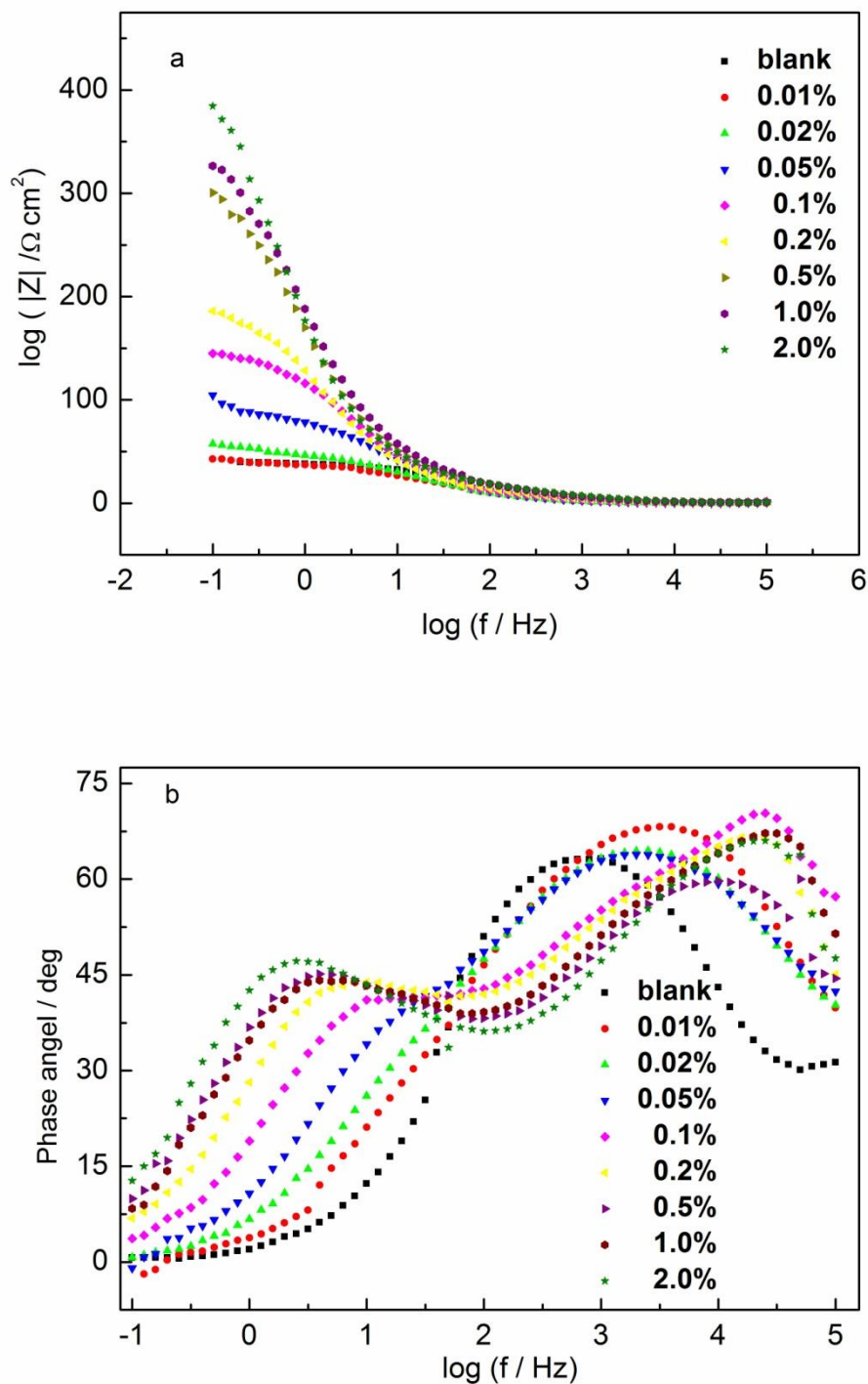


Figure 3. Bode plots of N80 steel in 15% HCl solution at 363K in the absence and presence of different concentrations of MB

A typical electrical equivalent circuit can be employed to analyze the impedance of absence and low concentrations of MB, as shown in Fig.4a. From the equivalent circuit, R_s is the electrolyte

resistance (Ωcm^2), R_t is the charge transfer resistance (Ωcm^2) and a constant phase element CPE ($\mu\text{F cm}^{-2}$) was used instead of an ideal capacitor. The CPE is described by expression:

$$\text{CPE} = \frac{1}{Q} \times \frac{1}{(j\omega)^n} \quad (3)$$

where Q is the CPE coefficient, ω is $2\pi f$, n has the meaning of phase shift and j is the imaginary unit.

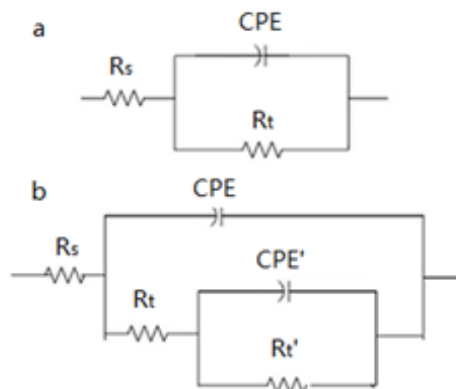


Figure 4. Electrical equivalent circuits for N80 steel in: a) blank acid and with low concentrations of MB (0.01%, 0.02%, 0.05% and 0.1%), b) with high concentrations of MB (0.2%, 0.5%, 1% and 2%)

Contrary to the situation observed in low MB concentrations, the Bode diagrams for concentrations above 0.1% clearly show the presence of a new phase angle shift. This new phase shift means that the formation of inhibitor film changed the electrode interfacial structure and resulted in an extra time constant. The presence of another time constant at high frequencies can be related to the higher coverage of adsorption film of MB inhibitor at metal/water interface due to the increase of concentration. Hence, a more complex equivalent circuit was introduced to analyze the impedance plots, shown in Fig. 4b.

Here, R_s is the electrolyte resistance ($\Omega\text{ cm}^2$), R_t is the resistance of the film (Ωcm^2), CPE ($\mu\text{F cm}^{-2}$) is related to the non-ideal capacitance of the inhibitor film, R_t' is the charge transfer resistance ($\Omega\text{ cm}^2$) and CPE' ($\mu\text{F cm}^{-2}$) is related to the non-ideal capacitance of the double layer of the bare metal. Table 2 shows various electrochemical parameters obtained by fitting the experimental data.

Two peaks in phase change vs. frequency plots indicate that there exist two electrochemical kinetic processes at the interface. The peak at low frequency would be due to corrosion electrochemical process. And the high frequency one can be attributed to the inhibitor film [24].

3.3 Weight loss measurements

Weight loss measurements were carried out to investigate the dissolution of N80 in 15% HCl solutions in the absence and presence of different concentrations of MB with different temperatures ranging from 303K to 363K. Fig. 5 shows corrosion rates and inhibition efficiencies calculated from

weight loss at different temperatures (303K, 323K, 343K and 363K) and concentrations of MB, ranging from 0 to 2% at 363K. The results show that, at every temperature, the corrosion rates decrease, while the corrosion inhibition efficiencies increase with the addition of the inhibitors, which indicate the high efficiency of MB in alleviating the corrosion of N80 steel in HCl solution. The results also can be attributed to the adsorption of MB molecules at steel/HCl solution interface.

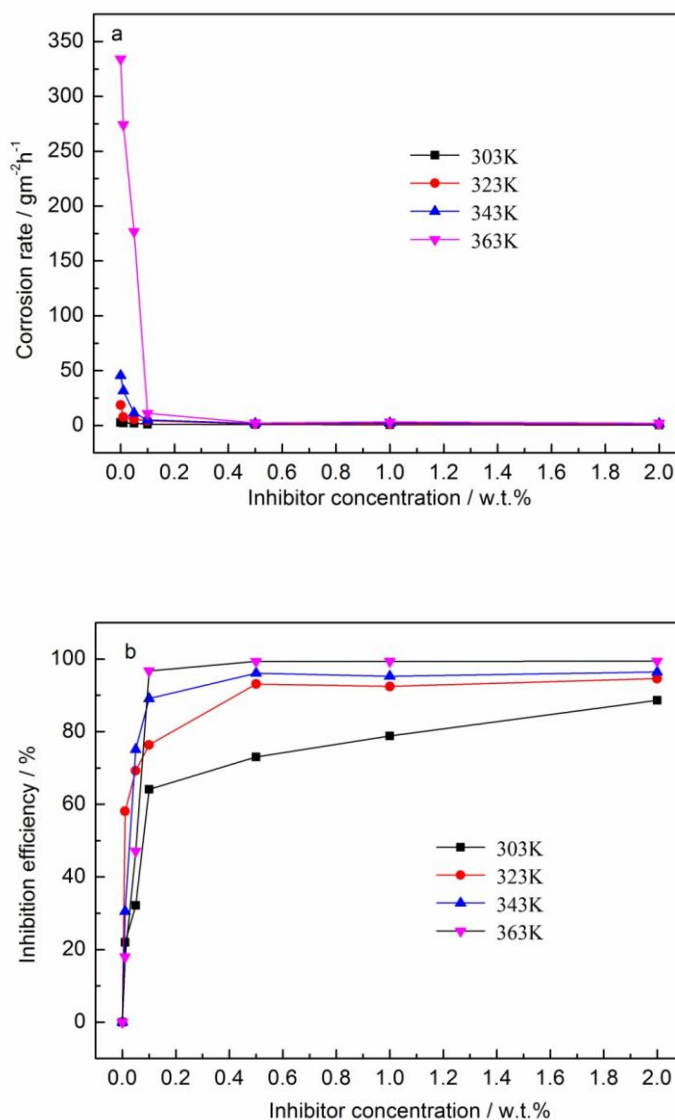


Figure 5. The variations of corrosion rates and inhibition efficiencies of N80 steel in 15% HCl solution in the presence of different concentrations of MB at different temperatures.

According to Arrhenius equation, the active energy for corrosion reaction can be calculated, expressed as follows:

$$C_R = A \exp\left(-\frac{E_a}{RT}\right) \tag{4}$$

where C_R is the corrosion rate from weight loss experiments, A is the pre-exponential factor, R is the gas constant, T is the absolute temperature and E_a is the Activation energy.

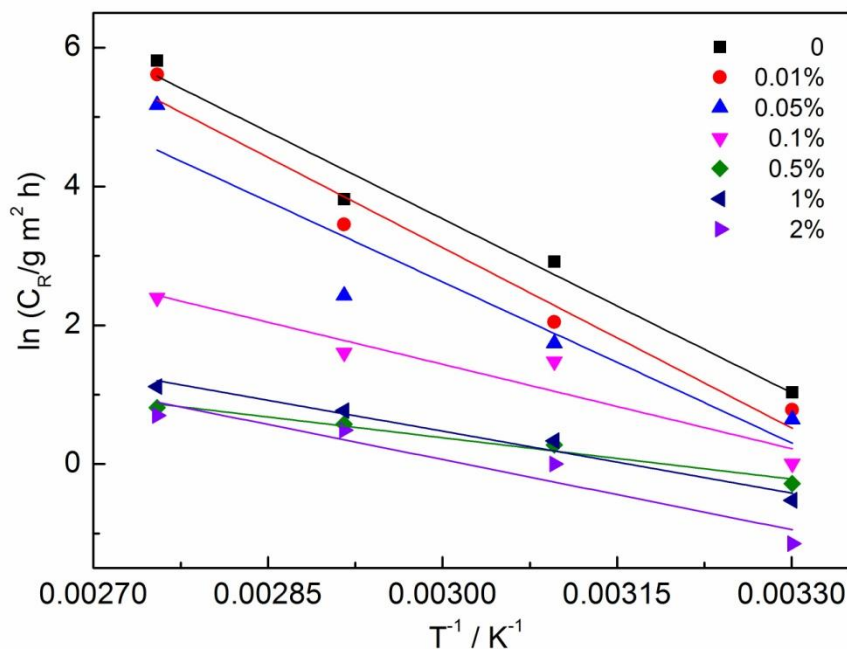


Figure 6. Arrhenius plots of N80 steel in 15% HCl solution in the absence and presence of different concentrations of MB.

The activation energy can be determined by linear regression between $\log C_R$ and $1/T$, shown in Fig. 6. And the results are listed in Table 2. All the linear regression coefficients at different concentrations are close to 0.95, indicating that N80 steel corrosion in 15% HCl solution can be elucidated to a reasonable degree of certainty using the kinetic model [24-27].

It is commonly believed that the effective energies of activation of corrosion process varied from 57.7-87.8KJ mol⁻¹ in hydrochloric acid solution, mostly grouped around 60.7kJmol⁻¹. [26] It is also proved that the presence of corrosion inhibitor in acidic solution would result in structural change of the double layer at the metal/water interface and reduced the rate of electrochemical reaction. Hence, the activation energy would probably reduce, which indicates the less possibility of electrochemical reaction process. It is shown in Table 3 that, in our study, the value of activation energy E_a is about 69.50kJ mol⁻¹ in the absence of MB inhibitor, which is in the range of above mentioned value. With the increase of MB inhibitor concentration, both E_a and pre-exponential factor A decrease apparently. The decrease of E_a can be explained as being indicative of chemisorptions. There exists the $Fe(Inhi)_{ads}$ intermediate on mild steel surface in the presence of corrosion inhibitor in acidic solution. A compact and coherent inhibitor overlayer would probably form on the metal surface and then reduced chemical attacks [28].

Table 3. Calculated activation energy E_a values for N80 corrosion rate in 15% HCl in the absence and presence of MB inhibitor

MB conc.(%)	E_a (kJ mol ⁻¹)	A(g m ⁻² h ⁻¹)
blank	69.50	28.62
0.01	70.05	29.13
0.05	64.29	25.83
0.1	33.68	13.60
0.5	19.51	6.34
1	24.67	9.38
2	25.99	10.17

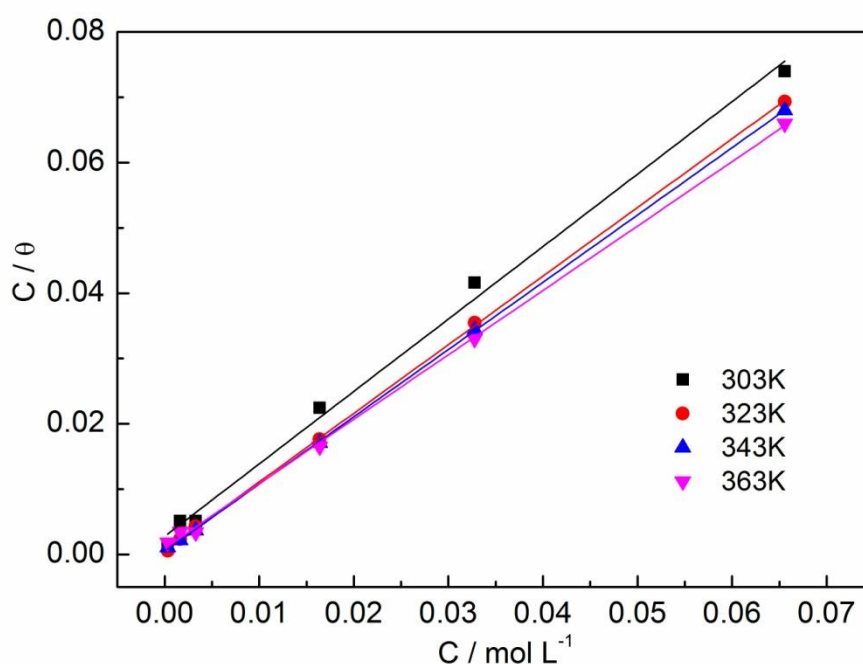


Figure 7. Langmuir adsorption of MB inhibitor on N80 steel in 15% HCl solution at different temperatures.

Several adsorption isotherms were fitted by the experimental data and the Langmuir adsorption isotherm was found to be the best expression of the adsorption behavior of MB inhibitor, which obeys the following equations:

$$\frac{C_{inh}}{\theta} = \frac{1}{K} + C_{inh} \tag{5}$$

$$K = \frac{1}{55.5} \exp\left(-\frac{\Delta G_{ads}^0}{RT}\right) \tag{6}$$

where C_{inh} is the inhibitor concentration, θ is the surface coverage and can be calculated from weight loss data, K is the adsorptive equilibrium constant, ΔG_{ads}^0 is the standard free energy of adsorption, R is the gas constant, T is the absolute temperature and the factor 55.5 is the water molar

concentration used to adjust the cratic contribution to the free energy of association of reactants [19, 29]

Fig. 7 shows the relationship between C/θ and C in the absence and presence of different concentrations of MB inhibitor at 303K, 323K, 343K and 363K, respectively. All the linear regression coefficients at different temperatures are more than 0.99, which indicates that the adsorption process can be expressed as Langmuir adsorption. The values of free energy (ΔG_{ads}^0) of adsorption at different temperatures are shown in Table 4. It is shown that all the ΔG_{ads}^0 values are negative, indicating the adsorption process of inhibitor onto N80 surface are spontaneous process. It is generally assumed that the adsorption mechanism can be determined by the value of free energy ΔG_{ads}^0 . ΔG_{ads}^0 values up to -20kJ/mol are assumed the as the electrostatic interaction between charged molecules and charged metal surface (physisorption). While ΔG_{ads}^0 values more negative than -40kJ/mol are considered as charge sharing or transfer from the inhibitor molecules to the metal surface to form a coordinate covalent bond (chemisorption). In our study, all the ΔG_{ads}^0 values are between -20kJ/mol and -40kJ/mol, which means the adsorption of MB inhibitor is neither typical physisorption nor typical chemisorption, but a complex mixed type.

Table 4. Calculated free energy ΔG_{ads}^0 values of MB inhibitor on N80 steel in 15% HCl at different temperatures.

T (K)	ΔG_{ads}^0 (kJ mol ⁻¹)
303	-24.94
323	-30.75
343	-33.30
363	-33.05

The adsorption of MB inhibitor on N80 surface in HCl solution involves both physisorption and chemisorptions. The ΔG_{ads}^0 values gradually increase with temperature, suggesting the stronger interaction between MB inhibitor and N80 steel surface at higher temperatures. It is also confirmed that the adsorption of MB inhibitor on N80 surface in HCl solution is complex but predominantly chemisorptions [12, 31].

3.4 Surface morphological examination

Fig. 8 shows the surface morphologies of N80 steel in the absence and presence of 2% MB inhibitor after immersed in 15% HCl solution for 4 hours at 363K. It can be seen that in the absence of MB inhibitor, Fig. 8a, the metal surface is badly corroded and apparently corroded appearance can be observed. The corrosion is caused by strong acid, HCl. Hydrogen depolarization reaction is the main reason for anodic dissolution.

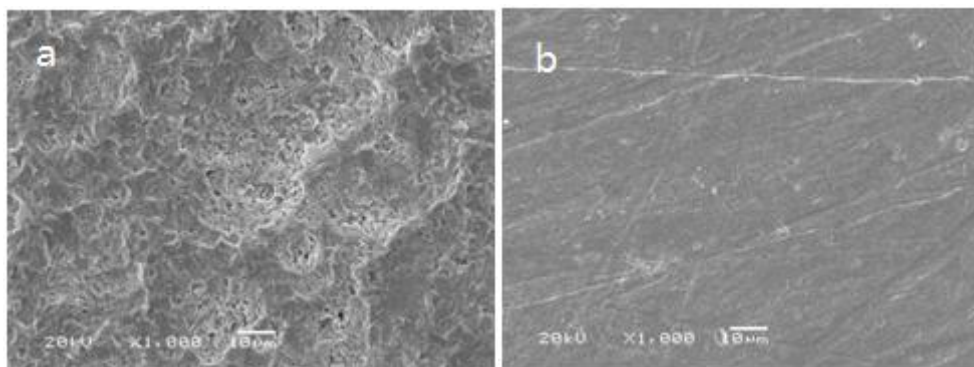


Figure 8. Surface morphologies of N80 steel by SEM after immersed in 15% HCl solution at 363K for 4 hours, a) in the absence of MB inhibitor, and b) in the presence of 2% MB corrosion inhibitor.

Therefore, the morphology also appears as uniform corrosion and no apparent localized corrosion can be observed. In the presence of 2% MB inhibitor, the metal surface is quite smooth and even the grooves induced by abrasion can be seen, shown in Fig. 8b. The metal surface was only slightly corroded in an extent of what SEM could not clearly distinguish. In brief, MB inhibitor is very efficient in protecting N80 steel in HCl environment.

4. CONCLUSIONS

Mannich base (MB) of 3-(diethylamino)-1-phenylpropan-1-one was synthesized and studied as an acidizing corrosion inhibitor for N80 steel in 15% HCl solution at different concentrations and temperatures. From the results, the following conclusions can be drawn:

(1) Polarization curves revealed that MB inhibitor is a mixed-type inhibitor in which both cathodic and anodic process of corrosion can be influenced by adsorption of MB molecules. Passivation region can be observed on anodic curves at high concentration of MB.

(2) EIS measurements showed that the concentration of MB inhibitor had pronounced impact on the electrochemical mechanism. In the presence of high concentrations of MB, two capacitive impedance loops and two time constants can be observed, indicating that there exist two electrochemical kinetic processes at the interface. One is for corrosion electrochemical process and the other corresponds to the inhibitor film.

(3) MB inhibitor has well pronounced inhibition properties in corrosion of N80 steel in hydrochloride acid at all temperatures. The fitting of weight loss data proved the adsorption is a complex mixed type, both physisorption and chemisorptions.

(4) SEM proved that MB inhibitor is highly efficient in preventing N80 steel from corrosion in HCl solution.

References

1. K. Lund, H. Fogler, C. McCune, *Chem. Eng. Sci.*, 28 (1973) 691.

2. K. Lund, H. Fogler, C. McCune, J. Ault, *Chem. Eng. Sci.*, 30 (1975) 825.
3. K. Lund, H. Fogler, C. McCune, *Chem. Eng. Sci.*, 30 (1975) 1325.
4. C. Cohena, D. Dinga, M. Quintard, B. Bazin, *Chem. Eng. Sci.*, 63 (2008) 3088.
5. J. Zhang, J. Zhao, N. Zhang, C. Qu, X. Zhang, *Ind. Eng. Chem. Res.*, 50 (2011) 7264.
6. M. Migahed, I. Nassar, *Electrochim. Acta*, 53 (2008) 2877.
7. M. Finšgar, J. Jackson, *Corros. Sci.*, 86 (2014) 17.
8. J. Gao, Y. Weng, Salitanate, L. Feng, H. Yue, *Pet. Sci.*, 6 (2009) 201.
9. G. Schmitt, *Br. Corros. J.*, 19 (1984) 165.
10. M. Morad, A. Kamal El-Dean, *Corros. Sci.*, 48 (2006) 3398.
11. M. Quraishi, D. Jamal, *Mater. Chem. Phys.*, 68 (2001) 283.
12. S. Vishwanatham, N. Haldar, *Corros. Sci.*, 50 (2008) 2999.
13. M. Quraishi, I. Ahamad, A. Singh, S. Shukla, V. Singh, *Mater. Chem. Phys.*, 112 (2008) 1035.
14. E. Flores, O. Olivares, N. Likhanova, M. Domínguez-Aguilar, N. Nava, D. Guzman-Lucero, M. Corrales, *Corros. Sci.*, 53 (2011) 3899.
15. I. Ahamad, R. Prasad, M. A. Quraishi, *Corros. Sci.*, 52(2010)1472.
16. E. Ferreira, C. Giancomelli, F. Giacomelli, A. Spinelli, *Mater. Chem. Phys.*, 83 (2004) 129.
17. D. Singh, S. Kuma, G. Udayabhanu, R. John, *J. Mol. Liq.*, 216 (2016) 740.
18. C. Rahal, M. Masmoudi, R. Abdelhedi, R. Sabot, M. Jeannin, M. Bouaziz, P. Refait, *J. Electroanal. Chem.*, 769 (2016) 56.
19. M. Fiori-Bimbi, P. Alvarez, H. Vaca, C. Gervasi, *Corros. Sci.*, 92 (2015) 192.
20. X. Li, S. Deng, G. Mu, H. Fu, F. Yang, *Corros. Sci.*, 50 (2008) 420.
21. D. López, S. Simison, S. de Sánchez, *Corros. Sci.*, 47 (2005) 735.
22. H. Zhang, X. Pang, M. Zhou, C. Liu, L. Wei, K. Gao, *Appl. Surf. Sci.*, 356 (2015) 63.
23. J. Cruz, R. Martínez, J. Genesca, E. García-Ochoa, *J. Electroanal. Chem.*, 566 (2004) 111.
24. Y. Tan, S. Bailey, B. Kinsella, *Corros. Sci.*, 38 (1996) 1545.
25. L. Yohai, M. Vázquez, M. Valcarce, *Electrochim. Acta*, 102 (2013) 88.
26. S. Martinez, I. Stern, *J. Appl. Electrochem.*, 31 (2001) 973.
27. A. Popova, E. Sokolova, S. Raicheva, M. Christov, *Corros. Sci.*, 45 (2003) 33.
28. J. de Damborenea, J. Bastidas, A. Vhquez, *Electrochim. Acta*, 42 (1997) 455.
29. S. Ali, H. Al-Muallem, S. Rahman, M. Saeed, *Corros. Sci.*, 50 (2008) 3070.
30. J. Zhao, G. Chen, *Electrochim. Acta*, 69 (2012) 247.
31. W. Li, Q. He, S. Zhang, C. Pei, B. Hou, *J. Appl. Electrochem.*, 38 (2008) 289.